

A case study of real-world tailpipe emissions for school buses using a 20% biodiesel blend

Claudio Mazzoleni ^{a,*}, Hampden D. Kuhns ^a, Hans Moosmüller ^a, Jay Witt ^{b,2},
Nicholas J. Nussbaum ^a, M.-C. Oliver Chang ^{a,1}, Gayathri Parthasarathy ^a,
Suresh Kumar K. Nathagoundenpalayam ^a, George Nikolich ^a, John G. Watson ^a

^a Desert Research Institute, Nevada System of Higher Education, 2215 Raggio Parkway, Reno, NV 89512, USA

^b Community Planning Association of Southwest Idaho, 800 S. Industry Way, Suite 100, Meridian, ID 83642, USA

Received 1 March 2007; received in revised form 18 May 2007; accepted 9 June 2007

Available online 30 July 2007

Abstract

Numerous laboratory studies report carbon monoxide, hydrocarbon, and particulate matter emission reductions with a slight nitrogen oxides emission increase from engines operating with biodiesel and biodiesel blends as compared to using petroleum diesel. We conducted a field study on a fleet of school buses to evaluate the effects of biodiesel use on gaseous and particulate matter fuel-based emission factors under real-world conditions. The field experiment was carried out in two phases during winter 2004. In January (phase I), emissions from approximately 200 school buses operating on petroleum diesel were measured. Immediately after the end of the first phase measurement period, the buses were switched to a 20% biodiesel blend. Emission factors were measured again in March 2004 (phase II) and compared with the January emission factors. To measure gaseous emission factors we used a commercial gaseous remote sensor. Particulate matter emission factors were determined with a combination of the gaseous remote sensor, a Lidar (light detection and ranging), and transmissometer system developed at the Desert Research Institute of Reno, NV, U.S.A. Particulate matter emissions from school buses significantly increased (up to a factor of 1.8) after the switch from petroleum diesel to a 20% biodiesel blend. The fuel used during this campaign was provided by a local distributor and was independently analyzed at the end of the on-road experiment. The analysis found high concentrations of free glycerin and reduced flash points in the B100 parent fuel. Both measures indicate improper separation and processing of the biodiesel product during production. The biodiesel fuels used in the school buses were not in compliance with the U.S.A. ASTM D6751 biodiesel standard that was finalized in December of 2001. The U.S.A. National Biodiesel Board has formed a voluntary National Biodiesel Accreditation Program for producers and marketers of biodiesel to ensure product quality and compliance with the ASTM standard. The results of our study underline the importance of the program since potential emission benefits from biodiesel may be reduced or even reversed without appropriate fuel quality control on real-world fuels.

© 2007 Elsevier B.V. All rights reserved.

Keywords: Real-world emissions; Biodiesel; Particulate; Pollution; Vehicles; Diesel; Fuel standard; Aerosols; Biofuels

* Corresponding author. Currently at Los Alamos National Laboratory, Division of International Space and Response, Remote Sensing Group, MS D436, Los Alamos, NM 87545, USA. Tel.: +1 505 665 9237; fax: +1 505 664 0362.

E-mail address: Claudio@lanl.gov (C. Mazzoleni).

¹ Currently at the California Air Resources Board, 9528 Tel Star Ave. El Monte, CA 91731, USA.

² Currently at WGI — Infrastructure 720 Park Blvd. Boise, ID 83729, USA.

1. Introduction

Biodiesel is an alternative, partially renewable source of energy prepared by the trans-esterification of vegetable oils or waste animal fats. It can be used in diesel engines without any engine modification (Graboski and McCormick, 1998). Its production and use are increasing rapidly, often aided by government subsidies designed to reduce emissions of criteria pollutants and net emissions of CO₂ (Economist, 2005). Biodiesel is composed of carbon extracted by the photosynthesis process from atmospheric CO₂ using solar radiation as an energy source. Use of biodiesel returns the carbon to atmospheric CO₂ during combustion and it reduces net CO₂ emissions into the atmosphere compared to the combustion of fossil fuel produced from sequestered fossil carbon from oil and gas deposits. The amount of energy required to produce biodiesel from its feedstock is a fraction of the combustion energy produced by the final product. Peterson and Hustrulid (1998) estimated that substituting ~50% of the entire U.S.A. transportation petroleum diesel (PD) fuel stock with rapeseed methyl ester (RME) or rapeseed ethyl ester (REE) biodiesel would result in a reduction of 113–136 billion kg of CO₂ per year released in the atmosphere. This could account for ~2–3% of fossil fuel CO₂ emissions in the U.S.A. (Marland et al., 2006). The effective CO₂ emission reduction depends on the fuel production process, raw material production, and transport which may vary between different industries, process methods, providers, and locations. DeWulf et al. (2005) calculated that the renewable fraction (meaning the total energy content in the fuel minus the energy contribution from non-renewable sources needed along all the production chain of the fuel divided by the total energy content) of RME, soybean methyl ester (SME) and corn-based ethanol (EtOH) biofuels are 67.6%, 65.8% and 75.7%, respectively.

Diesel engines emit substantial amounts of nitrogen oxides (NO_x, precursor to tropospheric ozone) and particulate matter (PM) that are harmful to human health, reduce visibility, and affect the earth's radiative balance by absorption and scattering of solar radiation (Jacobson, 2002; Pope et al., 2002). Of particular concern is the exposure of children to these and other exhaust pollutants. Recent studies demonstrated how vehicle self pollution may be a serious health concern for passengers (Behrentz et al., 2005; Marshall et al., 2005). For these reasons, it is important to study the emissions of diesel engines.

Previous studies show mostly reductions of carbon monoxide (CO), hydrocarbons (HC), and PM tailpipe emissions, with a slight increase in NO_x emissions from vehicles fueled by biodiesel and biodiesel blends com-

pared to those from vehicles fueled by PD. Biodiesel usage with respect to PD usage, generally reduces the soot fraction of PM. McCormick et al. (2001) studied the emissions from a heavy duty truck engine using biodiesel produced from various feedstocks and compared them with emissions from the same engine using a certified PD fuel. During this study PM emissions were found to be substantially lower for using biodiesel than for using PD, with the exception for methyl linoleate which produced significantly higher emissions (McCormick et al., 2001). Reduced soot fraction was also measured. The lower soot fraction and the PM emission reductions have been related to the oxygen content in the biodiesel fuel (Graboski and McCormick, 1998; Sharp et al., 2000). Generally, emissions are found to decrease more with higher biodiesel blend fractions (Peterson and Reece, 1996; Graboski and McCormick, 1998). For example, a recent U.S.A. EPA comprehensive document summarizing the results of many previous studies reports reductions of 10.1% in PM, 21.1% in HC and 11.0% in CO with an increase of 2.0% in NO_x for blends of 20% biodiesel and 80% PD (Environmental Protection Agency, U.S.A., 2002). All these studies however were performed on engine or chassis dynamometers under controlled laboratory conditions, or on individual vehicles using on-board emission measurement equipment (Peterson et al., 1999) to reduce confounding factors such as fuel quality, temperature and humidity variability, and to carefully control engine-operating mode. Prior to emission testing, fuels were subjected to quality analyses. When, analyses indicated the fuels were not in compliance with the appropriate specification (U.S.A. ASTM D975 for petroleum diesel and U.S.A. ASTM D6751 for biodiesel), the emission tests were not performed.

In the past, vehicle emission inventories were based mostly on laboratory results. Laboratory studies have been, and still are today, fundamental to elucidate vehicle emissions with high detail of information. However, often the direct use of laboratory-measured emission factors (even with complex driving cycles to emulate real driving conditions) in computational models has failed to accurately predict pollutant concentrations in highly impacted areas (National Research Council (U.S.A.). Committee on Vehicle Emission Inspection and Maintenance Programs, 2000). Similarly, beneficial effects of inspection and maintenance programs on urban air quality have been frequently overestimated (National Research Council (U.S.A.). Committee on Vehicle Emission Inspection and Maintenance Programs, 2001). Starting in the 70s, new approaches to measure vehicle emissions in real-world conditions were introduced; including tunnel studies, remote sensing systems,

road-side inspections, on-board measurement systems, chase studies etc. (e.g., Pierson and Brachazek, 1983; Bishop et al., 1989; Sagebiel et al., 1997; Frey et al., 2003; Walsh et al., 1996; Gertler and Pierson, 1996; Stedman, 1989) These new techniques provided an all-new suite of information and identified multiple inaccuracies with the prediction of pollutant concentrations when extrapolated solely from laboratory studies. Real-world conditions are in fact very complex resulting in a multitude of influential factors including but not limited to: a) poor vehicle maintenance and wear and tear, b) changes in environmental conditions such as temperature, humidity, pressure etc. c) vehicle tampering, d) effects of inspection and maintenance programs, e) non-normality of emission distributions over large fleets, f) fuel enrichment at high engine loads, g) fuel reformulation, additives, and fuel quality.

Biodiesel emission results have been based mostly on a large body of laboratory studies while real-world studies have been very limited or completely missing. Real-world studies have been fundamental for our understanding of non-biodiesel, on-road vehicle emissions, and they should also be used to test the applicability of laboratory biodiesel studies to the real world. The investigation of potential discrepancies between laboratory and real-world studies is expected to improve emission inventories and to enhance our understanding of relevant variables influencing such inventories.

Here, we present results from an experimental approach designed to measure real-world changes in on-road gaseous and PM emissions for an in-use fleet of school buses before and after a switch from winter PD fuel blend to a blend of 20% biodiesel and 80% PD (B20). Blended biodiesel is designated BXX, where XX represents the volume percentage of biodiesel fuel in the blend. The real-world conditions in this study were documented including odometer readings of the school buses, bus models, bus engine loads, maintenance records, environmental conditions (i.e. the winter atmospheric conditions), fuel type, and fuel quality.

2. Experimental section

The buses used in this study were originally operating on a winter fuel blend of 70% 2-D and 30% 1-D diesel fuels (phase I) and were then switched to a blend of 80% 2-D, 20% biodiesel and 0.1% anti-gelling additive (phase II). The 1-D fuel is usually used in winter to prevent the cold weather gelling of 100% 2-D. Bugraski et al. (2004) report a reduction of PM emissions up to a maximum of 12% by using 1-D respect to 2-D. Con-

sidering that the 1-D fuel used during our study was only 30% of the PD blend, it is reasonable to assume that the effect of 1-D on PM emissions would be on the order of a 4% reduction. During the summertime, diesel fleets run on 100% 2-D due to the lower cost. Therefore, the fuel switch studied during our campaign and here analyzed is representative of a realistic wintertime B20 fuel implementation.

The blending 2-D fuel in both phases was obtained from the same local provider. Fuel testing after the experiment indicated that the 2-D fuels were within the ASTM D975 specifications. The fuel change to B20 occurred with no engine modifications or fuel system alterations. Recent biodiesel usage guidelines (NREL, 2006) recommend changing fuel filters immediately prior to using biodiesel. The reasoning for this is that biodiesel can dissolve impurities trapped in the filter and impair engine performance.

As part of a pilot study, five of the school buses studied here had switched to B20 18 months prior to the fuel switch for the rest of the fleet. During both study phases, the engine block heater was plugged in to an outlet when buses were parked overnight.

2.1. Experiment set-up

We measured on-road gaseous and PM emission factors (EFs) of passing vehicles in Meridian, Idaho (U.S.A. on a dead end road with a school bus depot at its end. The experiment was carried out in two phases. During phase I (January 12th to 15th, 2004), the school buses used PD. On January 16th, 2004, the fuel storage tank at the bus depot was refilled with B20 from a local provider. The B20 was mixed at the distributor and trucked to the bus depot for delivery. Phase II took place during March 1st to 4th, 2004 to measure the changes in EFs resulting from the fuel switch. In the period elapsed between the two phases, the buses were driven an average of 3200 km each. This distance equates to 4 to 5 tank fillings per bus between phase I and II. The time elapsed during the two phases while the buses continued to be used regularly was intended to permit to the entire engine system to be flushed with the new fuel many times and to identify and reduce transient problems due to fuel system deposits dissolved by the biodiesel, such as clogging of fuel filters and/or injection systems. Table 1 reports a list of bus model year, type and maker.

2.2. Instrumentation

EFs were measured using a cross-plume vehicle exhaust remote sensing system (VERSS), which is

Table 1
School bus model year and engine type sampled during the study

Model year	Engine
1983	Detroit Diesel 8.2 L
1984	Detroit Diesel 8.2 L
1985	Detroit Diesel 8.2 L
1986	Detroit Diesel 8.2 L
1987	Detroit Diesel 8.2 L
1988	Ford Brazilian
1989	Detroit Diesel 8.2 L
1990	Cummins B-Series 5.9 L
1991	Cummins B-Series 5.9 L
1992	Cummins B-Series 5.9 L
1993	Cummins B-Series 5.9 L
1994	Cummins B-Series 5.9 L
1995	Cummins B-Series 5.9 L
1996	Cummins B-Series 5.9 L
1997	Cummins B-Series 5.9 L
1998	Cummins B-Series 5.9 L
1998	Cummins ISB-Series 5.9 L computer controlled
1999	Cummins ISB-Series 5.9 L computer controlled
2000	Cummins ISB-Series 5.9 L computer controlled
2001	Cummins ISB-Series 5.9 L computer controlled
2002	Cummins ISB-Series 5.9 L computer controlled
2003	Ford DT 466/International
2004	Caterpillar

composed of a commercial gaseous remote sensing system (Bishop and Stedman, 1996) and a recently developed ultraviolet Lidar (light detection and ranging)

and transmissometer PM sensor (Moosmüller et al., 2003). The VERSS system measures fuel-based EFs in grams of pollutant emitted per kilogram of fuel burned. The fuel-based EFs are calculated using a carbon mass balance to ratio the pollutant concentrations to the carbon concentrations (primarily CO₂, CO and hydrocarbons) in the exhaust (Bishop and Stedman, 1996; Moosmüller et al., 2003). Mass or volume ratios are the standard units for remote sensing systems in typical setting. This is due to the inherent characteristic of this type of measurement where an unknown fraction of the total plume is sampled and only pollutant ratios can be determined with good accuracy. However, we have access to recorded monthly-averaged fuel efficiencies for each individual bus measured in this study over the period January–March 2004. For easier comparison with dynamometer studies, we calculated distance-based EFs for those buses which were identified by their vehicle identification number. The caveat to this is that fuel efficiencies are averages over a long period (1 month) and may not represent the fuel efficiency in the instant of and at the engine load experienced during the remote sensing measurements and therefore the distance-based EFs are only approximate values. The distance-based EFs are reported in Table 2.

The PM remote sensor is based on ultraviolet (266 nm) backscatter Lidar and transmissometer

Table 2
Arithmetic averages and medians of school bus EFs ($\pm 68\%$ confidence limit) for carbon monoxide (CO), hydrocarbons (HC), nitrogen oxide (NO), and particulate matter (PM)

Pollutant	Statistic	PD			B20		
		Hot engine		Cold engine	Hot engine		Cold engine
		$(\text{g}_{\text{Pollutant}}/\text{kg}_{\text{Fuel}})^{\text{a}}$		$(\text{g}_{\text{Pollutant}}/\text{kg}_{\text{Fuel}})^{\text{a}}$	$(\text{g}_{\text{Pollutant}}/\text{kg}_{\text{Fuel}})^{\text{a}}$		$(\text{g}_{\text{Pollutant}}/\text{kg}_{\text{Fuel}})^{\text{a}}$
CO	Average	11.8 \pm 0.6	18.7 \pm 0.9	4.7 \pm 0.6	10.7 \pm 0.7	25 \pm 1	5.6 \pm 0.5
	Median	8.0 \pm 0.4	13.3 \pm 0.7	3.0 \pm 0.4	6.7 \pm 0.4	17 \pm 1	3.5 \pm 0.5
	Number	497	397	89	413	538	149
HC	Average	1.3 \pm 0.1	3.4 \pm 0.2	0.9 \pm 0.1	1.6 \pm 0.1	3.1 \pm 0.2	0.72 \pm 0.06
	Median	1.0 \pm 0.1	2.8 \pm 0.2	0.64 \pm 0.07	1.20 \pm 0.05	2.4 \pm 0.2	0.53 \pm 0.05
	Number	487	353	77	406	527	145
NO	Average	21.9 \pm 0.6	25.9 \pm 0.6	6.7 \pm 0.4	21.6 \pm 0.5	25.7 \pm 0.6	7.6 \pm 0.3
	Median	20.5 \pm 0.9	24.6 \pm 0.5	6.4 \pm 0.3	19.7 \pm 0.5	22.9 \pm 0.7	6.7 \pm 0.6
	Number	449	363	82	381	479	139
PM	Average	0.57 \pm 0.03	1.05 \pm 0.05	0.24 \pm 0.03	1.07 \pm 0.06	1.73 \pm 0.07	0.38 \pm 0.02
	Median	0.47 \pm 0.03	0.92 \pm 0.05	0.20 \pm 0.06	0.89 \pm 0.03	1.41 \pm 0.04	0.33 \pm 0.02
	Number	241	234	56	291	494	132

PD denotes petroleum diesel, B20 denotes a blend of 20% biodiesel and 80% PD. Distance-based emission factors for cold engine are reported in grams of pollutant per kilometer.

^a Fuel-based emission factors in grams of pollutants emitted per kilograms of fuel consumed.

^b These distance-based emission factors expressed in grams of pollutants emitted per kilometer of driven distance have been calculated assuming a fuel density of 0.8412 kg/L for petroleum diesel and of 0.8472 kg/L for B20 and using measured monthly fuel efficiencies for each bus. We calculated only cold-start distance-based emission factors because the buses were uniquely identified by their number only in the outbound direction (see “Site set-up” subsection). The need for unique identification also explains the smaller sample size. The average fuel efficiency for January 2004 was 2.9 km/L with a standard deviation of 0.9 km/L. The average fuel efficiency for March 2004 was 3.1 km/L with a standard deviation of 0.9 km/L.

technique. The transmission measurement is used to Lidar-invert optically dense plumes and to independently calculate PM emission factors. The Lidar and transmission systems have been discussed in detail elsewhere (Moosmüller and Keislar 2003; Moosmüller et al., 2003; Barber et al., 2004; Kuhns et al., 2004). However, the Lidar system used during the field campaign here described has been improved with respect to the previous system with a higher power laser, a larger telescope and a higher sensitivity photomultiplier, reaching a minimum detection limit of $0.06 \text{ g}_{\text{PM}}/\text{kg}_{\text{Fuel}}$ for an individual vehicle. The calibration procedure has been improved as well and higher precision and accuracy are reached. The collocated commercial gases remote sensor measures CO, HC, NO, and CO₂ column contents by non-dispersive infrared absorption. CO₂, CO, and HC measured by the gaseous remote sensor were used to calculate the fuel-based PM emission factors discussed here. A 200 ms measurement of the background of gases and PM column contents was performed immediately before each vehicle passage, while the measurement of the tailpipe emissions lasted for 500 ms immediately after each vehicle passage.

2.3. Site set-up

The emission samplers were located with a power generator on the south side of a dead end road at a school bus depot in Meridian, ID, U.S.A. Retro-reflectors for the gas and PM remote sensing units were aligned facing the transmitters and receiver units on the north side of the road. Traffic on the dead end street was restricted with traffic cones and road signs so that only one vehicle at a time passed by the sampling system. In addition to the school buses, each day, the school bus depot employees and the students and faculty of a local high school passed through the test section (inbound) with mostly spark ignition passenger vehicles that were hot stabilized from the commute. The vehicles were parked and left in parking lots for most of the day. Vehicles were identified and classified by acquiring a digital image with a camera as they passed through the site. Due to the orientation of the camera, license plates and bus identification numbers were only visible for vehicles leaving the bus depot. Inbound vehicles were classified by gross vehicle type such as car, pickup truck, bus, delivery truck, and SUV.

The distance between each individual vehicle parking spot and the sampling location ranged between 50 and 150 m for buses, and 100 and 250 m for non-bus vehicles. Both buses and private vehicles leaving the bus depot (outbound) had typically been parked for several

hours and their engines were operating under cold-start conditions (i.e., less than 2 minutes of engine operation after a 5+ hour cold soak). The vehicle driving direction was therefore associated with cold-start (outbound) and hot-stabilized (inbound) engine conditions.

2.4. Driving conditions

Driving speeds for the school buses through the system were similar during the PD and B20 tests. Outbound speeds averaged $11.1 \pm 0.5 \text{ km/h}$ and $10.3 \pm 0.3 \text{ km/h}$ and inbound speed averaged $11.4 \pm 0.3 \text{ km/h}$ and $10.7 \pm 0.3 \text{ km/h}$ for phases I and II, respectively. Acceleration values were more uncertain, but were generally small with an average of $1.3 \pm 0.4 \text{ km/(hs)}$. With these values and using the vehicle specific power formula described by Kuhns et al. (2004) and developed by Jimenez (1999) and by using typical gross vehicle weight and maximum power values for the school buses it is possible to estimate that on average the engines were operating at low load ($\sim 8\%$ to 16% of maximum power).

For privately owned vehicles outbound speeds averaged $16.9 \pm 0.2 \text{ km/h}$ and $16.5 \pm 0.2 \text{ km/h}$ and inbound speed averaged $19.8 \pm 0.5 \text{ km/h}$ and $19.1 \pm 0.4 \text{ km/h}$ for phases I and II, respectively. Accelerations were generally negative and small with an average of $-0.56 \pm 0.08 \text{ km/(hs)}$. The uncertainties reported here represent the standard error of the means (i.e. the standard deviation divided by the square root of the number of samples).

2.5. Data processing and analysis

We grouped EFs by vehicle type, model year, and driving direction. Due to the non-normality of emission distributions, average and median values and their statistical uncertainties were calculated for each group with the uncertainties defined as plus or minus half the interval between the 16%ile and 84%ile confidence limits of the distribution of 50,000 bootstrap estimates from randomly resampled (with replacement) sets of the data (Diaconis and Efron, 1983; Mazzoleni et al., 2004). For the average, this uncertainty corresponds to the standard error (i.e. the standard deviation divided by the square root of the number of samples).

2.6. Weather conditions

Weather conditions were recorded during the two phases with cold temperatures ($-7 \text{ }^\circ\text{C}$ to $0 \text{ }^\circ\text{C}$ for phase I and $-4 \text{ }^\circ\text{C}$ to $8 \text{ }^\circ\text{C}$ for phase II) and with relative

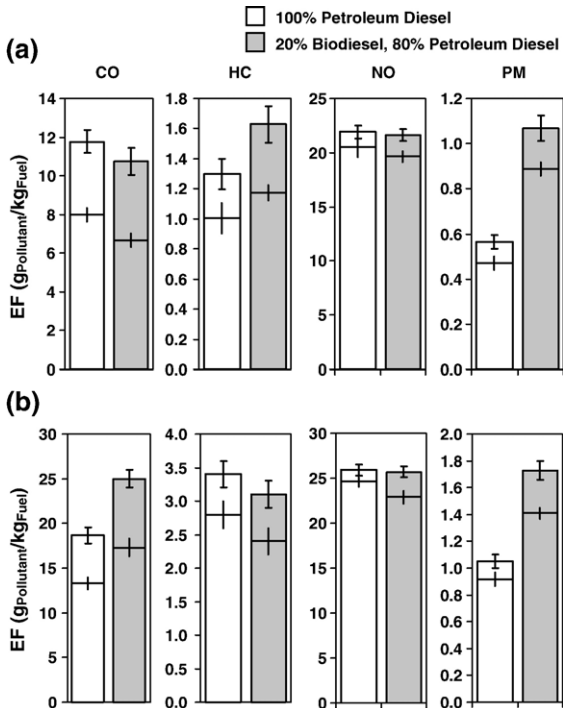


Fig. 1. Gases (CO, HC, NO), and particulate matter (PM) EFs for school buses tested in hot-stabilized and cold-start engine conditions. For each pollutant, the height of the column indicates the arithmetic average EF. The horizontal line across each column indicates the median EF. The vertical error bars represent the statistical uncertainties of the arithmetic averages and medians (68% confidence level). The number of samples for each average and median is reported in Table 2.

humidity ranging from 40% to 85%. A wintertime air stagnation event was occurring throughout phase I. Relative humidity was consistently higher in phase I than in phase II. However, a rain shower fell beginning on the evening of Wednesday of phase II and continued intermittently through Thursday. The precipitation did not affect the sampling systems; the elevated humidity did influence some of the measurements but did not bias the comparison, as described below.

3. Results and discussion

For all comparisons, a 2 sided *t*-test with alpha=0.05 was used to determine significant differences between phase I and II.

3.1. Overall school bus emissions

VERSS measurements showed that for school buses, the average cold-start CO EF was $34\% \pm 7\%$ higher after the switch to B20, while hot-stabilized CO EFs were not

significantly different. Cold-start HC EFs were indistinguishable based on fuel type but hot-stabilized HC EFs were $23\% \pm 11\%$ higher with B20. Changes of NO EFs were less than 1%. The largest changes in EFs were observed for PM. Cold-start PM EFs were $65\% \pm 8\%$ higher and hot-stabilized PM EFs were $88\% \pm 11\%$ higher after the buses had been switched to B20. Median EFs showed a similar pattern (Fig. 1 and Table 2). A comparison of quintile distributions for PM EFs showed that the difference between B20 and PD PM EFs was consistent over the entire fleet and not limited to only the highest emitting vehicles (Fig. 2). Choi et al. (1997) during a laboratory study on a 54 kW Caterpillar diesel engine also found increased PM emissions at low load (20% of maximum power) by using B20 relative to a baseline 2-D petroleum diesel fuel. However, the increase in emissions was generally smaller than the increase reported here. Similar conclusions can be deduced from the distance-based EFs (Table 2).

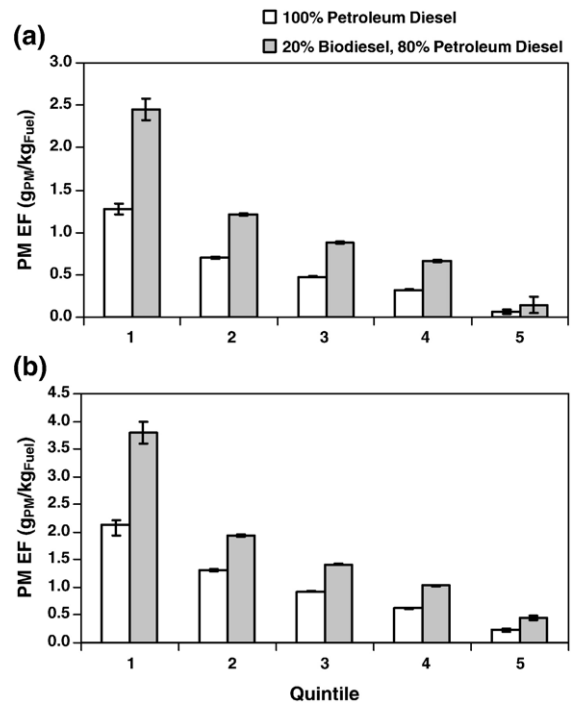


Fig. 2. Quintile distributions of particulate matter (PM) EFs for school buses with hot-stabilized and cold-start engine conditions. The PM EFs were sorted in decreasing order and divided into five equally sized groups, then for each group the arithmetic average was calculated. The error bars represent the uncertainties of the arithmetic averages (68% confidence level). Each hot-engine group includes 48 samples for PD and 58 samples for B20. Each cold-engine group includes 47 samples for PD and 99 samples for B20.

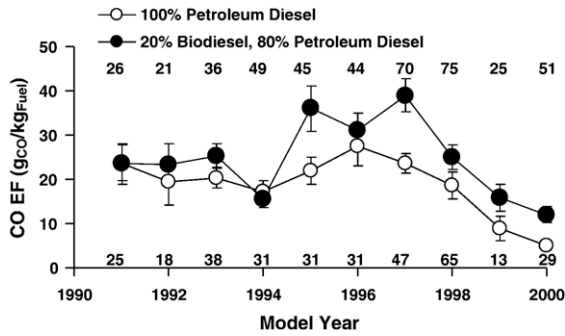


Fig. 3. Carbon monoxide (CO) arithmetic average EFs vs. model year for cold-start engine condition. Each point represents the arithmetic average EF in the respective model year bin. The error bars represent the uncertainties of the arithmetic averages (68% confidence level). The number of valid measurements for each year is shown above (B20) and below (PD) each data point. Overall arithmetic average CO EFs are: $19 \pm 3 \text{ g}_{\text{CO}}/\text{kg}_{\text{Fuel}}$ and $26 \pm 3 \text{ g}_{\text{CO}}/\text{kg}_{\text{Fuel}}$ for PD and B20, respectively.

3.2. Cold-start emissions

Significant increases of all EFs were measured for cold-start engine conditions with respect to hot-stabilized engine conditions (Fig. 1 and Table 2). The school buses did not have catalytic converters to reduce emissions once heated to a critical temperature. Increased EFs under cold-start conditions are known to be caused by non-ideal combustion conditions due to increased friction of moving parts that have yet to reach a thermal equilibrium, non-optimal viscosity of the lubricating oil, increased flame quenching on the cylinder walls, lower fuel vaporization at low temperature, and changed fuel–air mixture characteristics due to engine control system

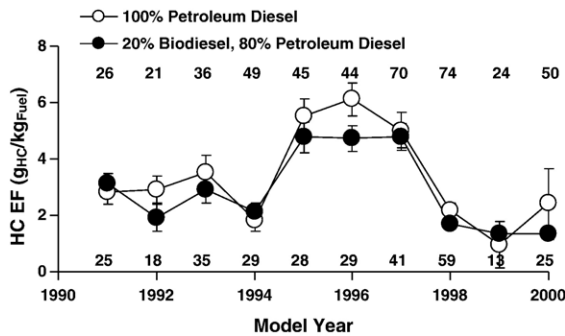


Fig. 4. Hydrocarbons (HC) arithmetic average EFs vs. model year for cold-start engine condition. Each point represents the arithmetic average EF in the respective model year bin. The error bars represent the uncertainties of the arithmetic averages (68% confidence level). The number of valid measurements for each year is shown above (B20) and below (PD) each data point. Overall arithmetic average HC EFs are: $3.4 \pm 0.6 \text{ g}_{\text{HC}}/\text{kg}_{\text{Fuel}}$ and $3.0 \pm 0.4 \text{ g}_{\text{HC}}/\text{kg}_{\text{Fuel}}$ for PD and B20, respectively.

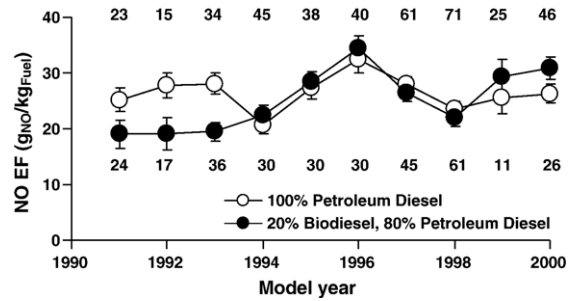


Fig. 5. Nitrogen oxide (NO) arithmetic average EFs vs. model year for cold-start engine condition. Each point represents the arithmetic average EF in the respective model year bin. The error bars represent the uncertainties of the arithmetic averages (68% confidence level). The number of valid measurements for each year is shown above (B20) and below (PD) each data point. Overall arithmetic average NO EFs are: $26 \pm 2 \text{ g}_{\text{NO}}/\text{kg}_{\text{Fuel}}$ and $26 \pm 2 \text{ g}_{\text{NO}}/\text{kg}_{\text{Fuel}}$ for PD and B20, respectively.

intervention to assure smooth engine operation in cold conditions (Heywood, 1988; Mathis et al., 2005).

Cold-start EFs were also related to school bus model year. Average CO, HC, NO and PM EFs grouped by model year showed a peak for model years 1995–1997. Lower EFs were measured with the newer buses. Since there were a limited number of buses in each model year, the uncertainty of average EFs from each single year was higher than the uncertainty of all 205 school buses in the fleet. When grouping by model year, differences between EFs from PD to B20 were generally small or not statistically significant for CO, HC, and NO (Figs. 3–5). PM EFs for buses running on B20 were significantly higher than EFs for buses running on PD for every model

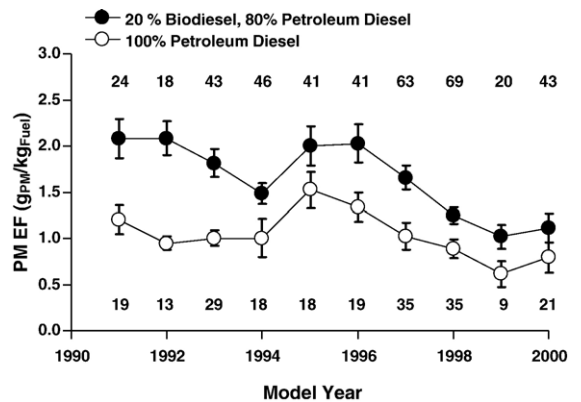


Fig. 6. Particulate matter (PM) arithmetic average EFs vs. bus model year for cold-start engine condition. Each point represents the arithmetic average EF in the respective model year bin. The error bars represent the uncertainties of the arithmetic averages (68% confidence level). The number of valid measurements for each year is shown above (B20) and below (PD) each data point. Overall arithmetic average PM EFs are: $1.04 \pm 0.05 \text{ g}_{\text{PM}}/\text{kg}_{\text{Fuel}}$ and $1.60 \pm 0.05 \text{ g}_{\text{PM}}/\text{kg}_{\text{Fuel}}$ for PD and B20, respectively.

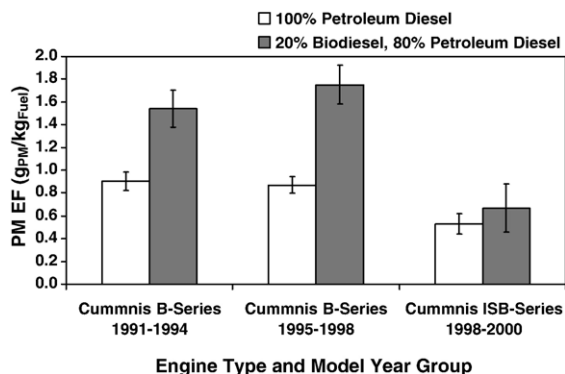


Fig. 7. Particulate matter (PM) arithmetic average EFs vs. bus engine type for cold-start engine condition. The error bars represent the uncertainties of the arithmetic averages (68% confidence level).

year tested with at least 9 valid measurements from each fuel (Fig. 6).

Engine type is generally a stronger factor that influences PM EFs than is vehicle model year. The dependence of PM EFs with engine type is analyzed in Fig. 7. To exclude the possible influence of steam on the PM measurements, the average EFs for the school buses were plotted vs. engine type only for vehicles with no visible steam (see “Effects of visible steam” subsection). The plot indicates that the average PM EFs are related to engine type. There are no evident physical differences between the Cummins B-Series engines from model years 1991–1994 and model years 1995–1998. Emissions were generally higher from the latter model year engines, so the results were stratified along what appeared to be a natural break in the data. The figure shows, the newer Cummins ISB-Series engines had lower PM EFs and were less prone to increased PM emissions when using B20. The ISB engine has a computer controlled fuel injection system and may have been able to compensate for restricted fuel flows associated with off-specification B20 Fuels.

Differences in the composition of the measured fleet during the two phases may have introduced a bias in the PM EFs comparison. To investigate this possibility, we calculated the number-weighted average PM EFs from the two phases for the same group of buses (only for buses identified by the video camera images, therefore only driven in the outbound direction, i.e., cold engine). The same bus was generally sampled in the outbound direction between 1 and 13 times with an average of ~5 times during the entire campaign. This analysis resulted in phase II (i.e., B20) arithmetic average and a median PM EF of 1.60 ± 0.04 g_{PM}/kg_{Fuel} and 1.36 ± 0.02 g_{PM}/kg_{Fuel}, respectively and phase I (i.e., PD) arithmetic average and a median PM EF of $1.05 \pm$

0.03 g_{PM}/kg_{Fuel} and 0.90 ± 0.04 g_{PM}/kg_{Fuel}, respectively. These results are nearly identical to the results reported for all buses with cold engines (Table 2).

3.3. Private vehicle emissions

EFs for bus district employees’ and high school students’ and faculty’s private vehicles were measured by VERSS during both study phases. We investigated the possibility of measurement biases due to instrumental or environmental changes between the two phases of the study by comparing EFs measured for these passenger vehicles (mostly gasoline cars, but also including a few vans, SUVs, and pickup trucks). Since these vehicles did not undergo a fuel switch or any other systematic change between study phases, they represent a control group for both study phases. PM EFs for hot-stabilized passenger vehicles did not change significantly between the two phases of the experiment (0.22 ± 0.03 g_{PM}/kg_{Fuel} (number of measurements $n=124$) in phase I and 0.18 ± 0.04 g_{PM}/kg_{Fuel} ($n=354$) in phase II). PM EFs for cold-start passenger vehicles increased marginally (with respect to the increase in the school buses emissions and with respect to the statistical uncertainties) during phase II (0.34 ± 0.04 g_{PM}/kg_{Fuel} ($n=264$) in phase I and 0.43 ± 0.04 g_{PM}/kg_{Fuel} ($n=483$) in phase II) (Table 3). Relative differences are far less than the school bus PM EF differences between phases. In a previous study (Mazzoleni et al., 2004) gasoline vehicle PM EF distributions have been found to be strongly skewed with up to 80% of gasoline vehicle fleet-averaged PM EF due to just 10% of the vehicles for hot engines. During

Table 3
Arithmetic averages and medians ($\pm 68\%$ confidence limit) of carbon monoxide (CO), hydrocarbons (HC), nitrogen oxide (NO), and particulate matter (PM) EFs for passenger vehicles

Pollutant	Statistic	Phase I		Phase II	
		(g _{Pollutant} /kg _{Fuel})		(g _{Pollutant} /kg _{Fuel})	
		Hot engine	Cold engine	Hot engine	Cold engine
CO	Average	25 ± 6	192 ± 15	49 ± 7	175 ± 10
	Median	4.0 ± 0.7	77 ± 7	4.0 ± 0.7	71 ± 7
	Number	216	312	394	552
HC	Average	3.8 ± 0.6	16 ± 1	3.2 ± 0.5	10.7 ± 0.6
	Median	1.3 ± 0.2	10.2 ± 0.6	0.8 ± 0.1	7.9 ± 0.4
	Number	189	273	371	525
NO	Average	1.5 ± 0.3	8.5 ± 0.6	1.5 ± 0.2	8.1 ± 0.4
	Median	0.8 ± 0.2	5.4 ± 0.5	0.7 ± 0.1	4.3 ± 0.5
	Number	152	219	347	502
PM	Average	0.22 ± 0.03	0.34 ± 0.04	0.18 ± 0.04	0.43 ± 0.04
	Median	0.16 ± 0.02	0.16 ± 0.02	0.06 ± 0.01	0.19 ± 0.02
	Number	124	264	354	483

the same study, only about 40% of the diesel fleet-averaged PM EF was due to highest emitting 10% of the diesel vehicles. This implies that gasoline high emitters generally dominate the averaged EFs; in addition these higher emitters have often highly variable emissions strongly influencing the average statistic. This is not true for diesel emissions at similar engine loads. These results support the conclusion that a systematic instrumental bias was not responsible for the large differences observed in the school bus PM EFs.

The relatively small difference between the school buses PM EFs and the passenger vehicles PM EFs is probably due to the fact that the school buses undergo constant and consisted maintenance while privately owned vehicles are often not well maintained. The model year data were unfortunately unavailable for the privately owned vehicles, however visual inspection suggested that a large fraction of the vehicles were old and not well maintained.

3.4. Effects of visible steam

Images of outbound vehicles indicated visible steam in the exhaust of ~22% of buses in phase I and 12% of buses in phase II. Visible steam was most frequent during cold mornings with high relative humidity. Average EFs for buses with visible steam were typically higher for CO, HC, and PM but lower for NO (Table 4). These results are consistent with the fact that normally only engines in cold-start condition show visible steam. The combustion conditions are non-ideal for cold engines, for which higher CO, HC, and PM and lower NO EFs are expected. However, school buses PM EFs were

significantly higher for B20 than for PD for exhaust with and without visible steam (Table 4).

3.5. Control buses emissions

Five “control” buses had been running on B20 since April 2003. The analysis of emissions from these buses provided another opportunity to test the consistency of the VERSS measurements for the two fuels. The control buses could only be identified by their number when driven in the outbound direction (cold engine). Arithmetic average PM EFs were comparable between the two study periods (1.62 ± 0.45 g_{PM}/kg_{Fuel} ($n=5$) in phase I vs. 1.76 ± 0.38 g_{PM}/kg_{Fuel} in phase II ($n=11$)). These EFs are similar to the average PM EF measured during phase II (B20) for the whole fleet (1.73 ± 0.07 g_{PM}/kg_{Fuel} ($n=494$)). The results were significantly higher than the average cold-engine PM EF measured for the buses using PD (1.05 ± 0.05 g_{PM}/kg_{Fuel} ($n=234$)) (Table 2). The agreement of the measured PM EFs for the control buses during the two phases and their elevated emissions with respect to the PD fueled buses add confidence that no instrumental or weather conditions changes substantially biased our results.

3.6. Effects of particle optical and physical properties on backscattering and extinction

The backscattering and extinction properties of particles depend on a multitude of parameters such as the material optical properties (e.g., complex refractive index of the particle components), on the mixing state of the particles (e.g., coated vs. uniformly mixed particles),

Table 4

Arithmetic averages and medians ($\pm 68\%$ confidence limit) of school bus EF for carbon monoxide (CO), hydrocarbons (HC), nitrogen oxide (NO), and particulate matter (PM) for steamer (Steam) and non-steamer (No Steam) vehicles

Pollutant	Statistic	PD (g _{Pollutant} /kg _{Fuel})			B20 (g _{Pollutant} /kg _{Fuel})		
		All	Steam	No Steam	All	Steam	No Steam
CO	Average	20 \pm 1	25 \pm 3	18 \pm 1	27 \pm 2	38 \pm 10	26 \pm 2
	Median	15 \pm 1	20 \pm 2	13 \pm 1	19 \pm 3	27 \pm 12	19 \pm 3
	Number	192	49	143	138	16	122
HC	Average	3.7 \pm 0.3	4.2 \pm 1	3.6 \pm 0.3	3.6 \pm 0.3	8 \pm 2	3.0 \pm 0.2
	Median	2.9 \pm 0.2	2.8 \pm 0.4	2.9 \pm 0.3	2.8 \pm 0.2	7 \pm 2	2.6 \pm 0.3
	Number	179	41	138	137	16	121
NO	Average	28.6 \pm 0.8	25 \pm 2	29.9 \pm 0.9	28 \pm 1	19 \pm 3	29 \pm 1
	Median	28 \pm 1	24 \pm 1	28.5 \pm 0.7	27 \pm 3	17.9 \pm 0.5	29 \pm 1
	Number	181	43	138	127	14	113
PM	Average	1.05 \pm 0.06	1.7 \pm 0.1	0.86 \pm 0.05	1.8 \pm 0.2	4 \pm 2	1.6 \pm 0.2
	Median	0.92 \pm 0.04	1.6 \pm 0.1	0.84 \pm 0.06	1.40 \pm 0.09	3.1 \pm 0.9	1.32 \pm 0.09
	Number	152	34	118	108	13	95

PD denotes petroleum diesel, B20 denotes a blend of 20% biodiesel and 80% PD. “All” indicates steamers and non-steamers together.

on the particle size distribution parameters (e.g., shape, mean diameter, spread), on the particle shape (e.g., spherical vs. fractal structure), etc. Additionally, backscattering and extinction mass efficiencies depend on particle bulk density. In particular, diesel emitted particles have a highly variable fraction of strongly absorbing carbon (generally denoted as black carbon) vs. lightly absorbing carbon (e.g. organics) compounds. Bulk material real and imaginary index of refraction directly depends on the fraction of absorbing vs. lightly absorbing components, which conversely influence scattering and absorption properties of particles. Therefore, the black carbon fraction of emitted particle controls the backscattering and extinction properties of the particle ensembles probed by the laser beam. The variability of these parameters adds another possible source of bias to the PM EFs inferred from the Lidar and transmissometer systems. The sensitivity of the backscattering mass efficiency used by the Lidar system to calculate the PM EFs has been theoretically investigated by Barber et al. (2004), who report changes in the backscattering mass efficiency of +38% for a reduction of the size distribution mass median diameter of 17%, and +12% for an increase in the real part of the index of refraction of 3.3% or a decrease in black carbon volume fraction of 20%, or an increase in size distribution geometric standard deviation of 17%, and –25% for an increase of mass median diameter of 17% or a decrease in size distribution geometric standard deviation of 17%.

Previous studies (Bagley et al., 1998; Krahl et al., 2003) showed a slight shift of the accumulation mode to smaller sizes for particles emitted by biodiesel-powered vehicles. In addition, as mentioned above, the black carbon fraction in the PM emissions is generally reduced with biodiesel and biodiesel blend use (Graboski and McCormick, 1998; Sharp et al., 2000). Following Barber's calculation, this would result in an increased backscattering mass efficiency up to +50%, for a decrease of mass mean diameter of 17% and a reduction in black carbon of 20%. Thus, using the same efficiency calculated for PD would result in an overestimation of the PM emitted by the biodiesel up to 20%. However, it is difficult to quantify the changes in size distributions and the effect on the measurements for our case, where the fraction of biodiesel in the blend used is much smaller (B20 vs. B100) and the particle characteristics may have been influenced by the off-specification fuel.

Barber et al. also report the sensitivity of the laser extinction mass efficiency to size distribution parameters and PM optical properties. Extinction mass efficiency is considerably less sensitive to changes of optical properties and/or size distribution: +8% for a decrease in

size distribution geometric standard deviation of 17% or an increase in the real part of the index of refraction of 3.3%, –8% for an increase in size distribution geometric standard deviation of 17% or a decrease in black carbon volume fraction of 20%. Therefore, PM EFs derived by extinction would have been underestimated by up to 4% if the black carbon fraction would have been decreased by 20% and the mass mean diameter would have been decreased by 17%. The maximum change is very small and in the opposite direction of the changes in the backscattering-based emission calculations. PM EFs derived from our ultraviolet extinction measurement however were much noisier than the PM EFs measured by the Lidar. One main problem with extinction measurements is that the quantity measured is generally small and is calculated from the difference between two much larger values (measured transmission in the tail-pipe plume minus the background light transmission). In addition, the extinction measurements performed during our study suffered from a positive bias due to air turbulence (caused by the vehicle air drag and the temperature difference between environment and plume exhaust) and/or instrumental vibration at the vehicle passage. A comparison between Lidar and extinction accuracies have been discussed in a previous paper (Mazzoleni et al., 2004).

Despite these uncertainties, the arithmetic average PM EFs for hot engine from the extinction channel were $1.74 \pm 0.16 \text{ g}_{\text{PM}}/\text{kg}_{\text{Fuel}}$ ($n=241$) and $3.61 \pm 0.34 \text{ g}_{\text{PM}}/\text{kg}_{\text{Fuel}}$ ($n=289$) while median PM EFs were $1.11 \pm 0.08 \text{ g}_{\text{PM}}/\text{kg}_{\text{Fuel}}$ and $1.72 \pm 0.13 \text{ g}_{\text{PM}}/\text{kg}_{\text{Fuel}}$ for PD and B20 respectively. A few outliers in the range of $50 \text{ g}_{\text{PM}}/\text{kg}_{\text{Fuel}}$ influenced the arithmetic averages, but had less effect on the medians. Both arithmetic averages and medians are larger for B20 than PD. For comparison on the same sample of buses, the Lidar channel measured the following EFs: arithmetic averages $0.57 \pm 0.03 \text{ g}_{\text{PM}}/\text{kg}_{\text{Fuel}}$ and $1.06 \pm 0.05 \text{ g}_{\text{PM}}/\text{kg}_{\text{Fuel}}$ and median EFs $0.47 \pm 0.03 \text{ g}_{\text{PM}}/\text{kg}_{\text{Fuel}}$ and $0.89 \pm 0.03 \text{ g}_{\text{PM}}/\text{kg}_{\text{Fuel}}$ for PD and B20, respectively. The increase in PM EFs measured by the extinction method after the fuel switch to the B20, combined with the small sensitivity of the extinction measurement to particle optical properties and size distribution, suggests that the increased EFs measured by Lidar have not been the result of a change in particle characteristics, but are effectively related to an increase in the PM EFs.

3.7. Validation of Lidar results

For a subset of the phase II measurements, we could evaluate the PM VERSS accuracy by using the results of

an extractive in-plume sampling system also deployed in the field. While a detailed discussion of the in-plume system and of the system comparison is beyond the scope of this paper, a brief description is given. The in-plume system has an inlet (a tube set-up on the lane center and covered by a cable protector) secured in the center of the road to sample the vehicle emissions. The sampled air is continuously drawn through the inlet to instruments that analyze it for both gasses and particles in real time. The particle mass is calculated from the volume size distribution measured in real time with a Dekati Electric Low Pressure Impactor (ELPI).

An FTIR spectrometer is used for gaseous species measurement, and a LiCor analyzer for CO₂ measurement. The in-plume fuel-based EFs are calculated by rationing the PM and gaseous sample concentrations to the CO₂ concentrations after a background subtraction. When well distinguishable individual peaks in the CO₂ concentration are identified and associated with specific vehicles, it is possible to calculate the individual vehicle PM EF and to compare it with the Lidar-based PM EF. The averaged PM EFs measured by the two systems compared well for both diesel (difference between averaged EFs measured by the two systems were <10%) and gasoline vehicles (<20%). Due to the high traffic conditions, it was difficult to clearly identify individual vehicle emissions measured by both systems. Therefore, to provide a statistically robust time comparison between the two systems, we calculated half-hour averaged PM EFs measured on March 4th, 2004 by the two systems. Fig. 8 shows the time series. Despite the uncertainties introduced by the difficulties of this comparison (including vehicle mismatching between the two systems) we found reasonable agreement between the in-plume and the VERSS. A linear regression analysis of VERSS vs. in-plume half-hour PM EFs yielded a slope of 0.7 ± 0.1 , an intercept of $0.2 \pm$

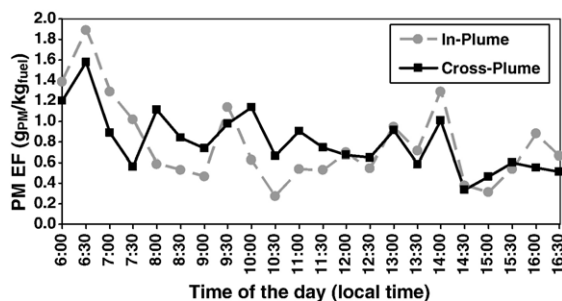


Fig. 8. Time series for in-plume and VERSS systems for half-hour averaged PM EFs for the 4th of March 2004. Overall average PM EFs are 0.78 ± 0.09 g_{PM}/kg_{Fuel} and 0.80 ± 0.06 g_{PM}/kg_{Fuel} for VERSS and in-plume system, respectively.

0.2 and a correlation coefficient R^2 of 0.5 ± 0.2 . The VERSS data compared well with the ELPI, which is a more established particle measurement method. A comparison between ELPI and gravimetric filter measurements is reported in a recent study by Maricq et al. (2006). The quality of the comparison depended on the method used to retrieve the PM mass and was influenced by an artifact overestimating the coarse particle counts. In our comparison, we avoided the influence of the coarse particle artifact by quantifying only particles with a diameter smaller than $0.59 \mu\text{m}$.

This assumption should be appropriate for diesel aerosol size distributions since most of the mass is in the ultrafine and accumulation mode. Zervas et al. (2005) reported good reproducibility and repeatability of emission tests using an ELPI as a real time particle sensor. The agreement between the in-plume and VERSS measurements adds confidence in the accuracy of the backscattering mass efficiency used in this study to convert the backscattering signals into particle mass concentrations.

Finally, a comparison between previous on-road results from our PM VERSS and a variety of other on-road and dynamometer PM measurements has been reported previously. The PM EFs for heavy duty diesel vehicles from different studies were distributed over a range of values (~ 0.6 to 2.5 g_{PM}/kg_{Fuel}) and our averaged PM VERSS EFs (1.3 to 2.1 g_{PM}/kg_{Fuel}) fell in this range (Mazzoleni et al., 2004).

3.8. Fuel analysis

Biodiesel may act as a solvent that dislodges deposits in the engine fuel delivery system. Maintenance records for the Meridian School District bus fleet from December 2003 through March 2004 indicated seven incidents of failed lift pumps or fuel injector pumps in the fleet of in-use buses (Table 5). The fuel pump failure that occurred on December 9, 2003 happened to one of the five buses that had been running on B20 for more than 1.5 years as part of a pilot project. With the exception of the one injector pump failure that occurred on January 9, 2004, all fuel system failures occurred after the buses had switched to B20. These mechanical problems and the PM EF results prompted the analysis of the fuels used in the buses during the study. Samples of B20 and B100 were collected from local distribution points and analyzed for their major components (Caleb Brett Laboratories Deer Park, Texas).

The analysis found that the B100 biodiesel available in the region had levels of free glycerin in excess of 0.05% by weight. The newly formulated ASTM (American Society for Testing and Materials) D6751

Table 5

List of mechanical problems with the school bus fleet between December 2003 and April 2004

Bus model year	Time on B20	Failure date	Driver complaint	Correction
2002	1.5 years	09-Dec-2003	Low power	Replaced fuel pump
1995	None	09-Jan-2004 (prior to fuel switch)	Injector pump failure	Replaced fuel line and fuel pump
1999	7 days	22-Jan-2004	Engine would not start	Replaced lift pump and fuel pump
1999	29 days	13-Feb-2004	Shut down on road. Blue smoke coming from exhaust	Replaced fuel pump
2001	75 days	15-Mar-2004	N/A	Replaced lift pump
1995	79 days	19-Mar-2004	Hard starting. No PSI building in fuel pump	Repaired/replaced fuel pump. Valve rechecked
1999	84 days	24-Mar-2004	Injector pump failure	Replaced injection pump and transfer pump

biodiesel standard (Table 6) requires free glycerin levels to be below 0.02% by weight. Free glycerin accounted for more than 50% of the measured total glycerin in the B100 fuels. In addition, the flash point of one of the B100 samples collected at a local distributor was 61 °C (less than the 130 °C lower limit in ASTM D6751).

There is currently no ASTM standard for B20 fuel. However, the lack of compliance of the parent B100 feedstock with ASTM D6751 may be inferred based on the results of the B20 analysis. If a biodiesel specific compound in the B20 exceeds 20% of the B100 ASTM standard, then it is highly likely that the B100 used for blending is non-compliant with ASTM D6751. While glycerin is a major byproduct of the trans-esterification

process used to make biodiesel, PD fuels have negligible levels of glycerin. Based on the assumption that there is no glycerin in the PD, the B100 parent fuel of the analyzed B20 had a free glycerin concentration of 0.1 mg/L and a total glycerin concentration of >1.0 mg/L, more than 5 times the ASTM D6751 standards.

The glycerin standards in ASTM D6751 are intended to prevent glycerin from collecting in fuel filters and clogging fuel injectors. Elevated free glycerin levels are caused by failure to completely separate the glycerin byproduct from the biodiesel product during the manufacture. Total glycerin is the sum of free and bound glycerin. Bound glycerin is typically associated with unreacted oils and fats from the original feedstock. A low

Table 6

Analysis of two B100 samples from regional distributors and B20 fuel (with anti-gelling additive) used by the school bus fleet in Meridian Boise, ID

Property	Unit	ASTM B100 Specification	D6751	B100#1	B100#2	B20
Copper corrosion		<3		1a ^a	1a ^a	1a ^a
Cloud point	°C	Must be reported		-12	-5	-6
Average micro carbon residue	wt.%	<0.05		<0.1 ^b	<0.1 ^b	0.09
Particulate arsenic	µg/L			<0.07	<0.03	<0.003
Particulate cadmium	µg/L			<0.02	<0.005	<0.0006
Particulate chromium	µg/L			3.3	<0.005	<0.0006
Particulate sodium	µg/L			367	181	72
Particulate lead	µg/L			47	<0.03	<0.003
Particulate calcium	µg/L			232	171	25
Particulate vanadium	µg/L			4.4	1.1	0.8
Particulate aluminum	µg/L			407	9	9
Particulate silicon	µg/L			71	8.8	4.1
Particulate iron	µg/L			6058	54	2.5
Total particulate contamination	mg/L			132	44	5.6
Free glycerin	wt.%	<0.02		>0.05	>0.05	0.02
Total glycerin	wt.%	<0.24		0.07	0.1	>0.2
Average acid number	mg KOH/g	<0.50		0.29	0.21	<0.05
Sulfate ash	wt.%	<0.020		<0.005	<0.005	<0.005
Corrected flash point	°C	>130.0		61	>110 ^b	66

The off-specification parameters are in bold.

^a In a copper corrosion test, copper strips are immersed into the oil being evaluated. At the end of the exposure period, the strips are removed and cleaned. The strips are compared to standardized reference strips and rated on a scale of class 1a,b (slight tarnish) to class 4a,b,c (heavy tarnish). The result 1a indicates marginal corrosion.

^b Inconclusive compliance with respect to ASTM D6751.

flash point is an indicator of unreacted alcohol remaining after processing of the feed stock oil. Both the free glycerin and low flash point measurements for the B20 indicate that the B100 parent fuel was not in compliance with the ASTM D6751 fuel quality standard.

Excess glycerin in the fuel has been previously shown to cause fuel system failure and poor combustion characteristics (NREL, 2006). Therefore, the use of off-specification fuel is likely to have contributed to the increase PM EFs in this study. During a recent survey of 27 USA biodiesel samples it was found that 85% of the samples met the ASTM D6751 requirements even if only one sample met the European oxidation stability requirement. The remaining 15% samples were non-compliant with U.S.A. standard for at least one regulated fuel property, this is a small but not negligible fraction of the biodiesel sold in U.S.A. (McCormick and Lawrence, 2004).

4. Conclusions and recommendations

The current study differs from previous controlled laboratory studies in that the effects of the fuel switch were tested on an entire in-use fleet under real-world conditions using commercially available fuels. Our results show that the use of off-specification B20 fuel instead of 100% PD substantially increased PM emissions. Cold-start CO emissions and hot-stabilized HC emissions were also higher with B20. Other tailpipe emissions were not significantly different.

The real-world conditions encountered in this study included use of commercial biodiesel that in retrospect did not meet ASTM D6751 biodiesel standards. This fact emphasizes the need for stringent quality control in the production of biodiesel. To this end, the U.S.A. National Biodiesel Board has recently formed a voluntary National Biodiesel Accreditation Program for producers and marketers of biodiesel to ensure product quality and compliance with the ASTM standard. Biodiesel consumers should seek vendors who have achieved certification through this program if they wish to maintain vehicle reliability and reduce exhaust emissions.

This study corroborates the necessity to always verify laboratory results in real-world conditions if we want to take full advantage of new technical advancements and fuels. In the past, remote sensing and other real-world measurement techniques, such as tunnel studies, have been successfully used in understanding the causes for the poor effectiveness of inspection and maintenance programs and poor accuracy of mobile emission models. Similarly, today it is important to use these techniques to evaluate the effectiveness of new fuels in reducing pollutants in the real-world. The

remote sensing system results provided us with an evidence of emission increase, and also guided us in understanding the most probable cause for the failure in reducing PM emissions with this fuel switch. Real-world data analysis represents not only an important scientific research tool but also a method to assure the quality of new commercial fuels and the adherence to fuel standards.

Acknowledgments

We thank Sue Johnston, Randy Owens, and the entire staff of the Meridian Joint School District No. 2 Transportation Department, the Meridian Joint School District No. 2 Bus Drivers, the Idaho Transportation Department, Yancey Willis and the rest of the Community Planning Association of Southwest Idaho, the Ada County Highway District, Angel Fontenot-Staley, Intek Caleb Brett, Dale Johnston of United Oil, and Dick Larson of Idaho Department of Water Resources (retired). The Strategic Environmental Research and Development Program (Contract CP-1336), and the Federal Transit Administration (Contract 26-70030) supported the instrument development.

References

- Bagley ST, Gratz LD, Johnson JH, McDonald JF. Effects of an oxidation catalytic converter and a biodiesel fuel on the chemical, mutagenic, and particle size characteristics of emissions from a diesel engine. *Environ Sci Technol* 1998;32(9):1183–91.
- Barber PW, Moosmüller H, Keislar RE, Kuhns HD, Mazzoleni C, Watson JG. On road measurement of automotive particle emissions by ultraviolet Lidar and transmissometer: theory. *Meas Sci Technol* 2004;15(11):2295–302.
- Behrentz E, Sabin LD, Winer AM, Fitz DR, Pankratz DV, Colome SD, et al. Relative importance of school bus-related microenvironments to children's pollutant exposure. *J Air Waste Manage Assoc* 2005;55(10): 1418–30.
- Bishop GA, Stedman DH. Measuring the emissions of passing cars. *Acc Chem Res* 1996;29:489–95.
- Bishop GA, Starkey JR, Ihlenfeldt A, Williams WJ, Stedman DH. IR long-path photometry: a remote sensing tool for automobile emissions. *Anal Chem* 1989;61(10):671A–7A.
- Bugraski A, Schanakenberg G, Noll J, Mischler S, Patts L, Hummer J, et al. The effectiveness of selected technologies in controlling diesel emissions in an underground mine — isolated zone study at Stillwater Mining Company's Nye Mine. Final report to metal/nonmetal diesel partnership; 2004. Accessed on-line on June 7th 2006 at <http://www.msha.gov/01-995/dpmdocs/stillwater.pdf>.
- Choi CY, Bower GR, Reitz RD. Effects of biodiesel blended fuels and multiple injections on D. I. diesel engines. *SAE Tech Pap* 1997;970218.
- DeWulf J, van Langenhove H, van de Velde B, DeWulf J, van Langenhove H, van de Velde B. Energy-based efficiency and renewability assessment of biofuel production. *Environ Sci Technol* 2005;39(10):3878–82.

- Diaconis P, Efron B. Computer-intensive methods in statistics. *Sci Am* 1983;248(5):116&.
- Economist T. Biofuels: stirrings in the corn fields. *Economist* 2005;375(8426):71–3.
- Environmental Protection Agency, U. S. A comprehensive analysis of biodiesel impacts on exhaust. EPA; 2002. Available on-line: <http://www.epa.gov/otaq/models/analysis/biodsl/p02001.pdf>.
- Frey HC, Unal A, Roupail NM, Colyar JD. On-road measurements of vehicle tailpipe emissions using a portable instrument. *J Air Waste Manage Assoc* 2003;53(8):992–1002.
- Gertler AW, Pierson WR. Recent measurements of mobile source emission factors in North American tunnels. *Sci Total Environ* 1996;189/190:107–13.
- Graboski MS, McCormick RL. Combustion of fat and vegetable oil derived fuels in diesel engines. *Prog Energy Combust Sci* 1998;24(2):125–64.
- Heywood JB. Internal combustion engine fundamentals. New York, NY: McGraw Hill; 1988.
- Jacobson MZ. Control of fossil-fuel particulate black carbon and organic matter, possibly the most effective method of slowing global warming. *J Geophys Res-Atmos* 2002;107(D19).
- Jimenez JL. Understanding and quantifying motor vehicle emissions with vehicle specific power and TILDAS remote sensing, Ph.D. Thesis. Massachusetts Institute of Technology 1999.
- Krahl J, Munack A, Schröder O, Stein H, Bünger J. Influence of biodiesel and different designed diesel fuels on the exhaust gas emissions and health effects. *SAE Techn Ser* 2003;2003-01-3199:2–9.
- Kuhns HD, Mazzoleni C, Moosmüller H, Nikolic D, Keislar RE, Barber PW, et al. Remote sensing of PM, NO, CO and HC emission factors for on-road gasoline and diesel engine vehicles in Las Vegas, NV. *Sci Total Environ* 2004;322(1–3):123–37.
- Maricq MM, Xu N, Chase RE. Measuring particulate mass emissions with the electrical low pressure impactor. *Aerosol Sci Technol* 2006;40(1):85–96.
- Marland G, Boden TA, Andres RJ. Global, regional, and national fossil fuel CO₂ emissions. Trends: a compendium of data on global change. Oak Ridge, Tenn., U.S.A.: Carbon Dioxide Information Analysis Center, Oak Ridge National Laboratory, U.S. Department of Energy; 2006.
- Marshall JD, Behrentz E, Marshall JD, Behrentz E. Vehicle self-pollution intake fraction: children's exposure to school bus emissions. *Environ Sci Technol* 2005;39(8):2559–63.
- Mathis U, Mohr M, Forss AM. Comprehensive particle characterization of modern gasoline and diesel passenger cars at low ambient temperatures. *Atmos Environ* 2005;39(1):107–17.
- Mazzoleni C, Kuhns HD, Moosmüller H, Keislar RE, Barber PW, Robinson NF, et al. On-road vehicle particulate matter and gaseous emission distributions in Las Vegas, Nevada, compared with other areas. *J Air Waste Manage Assoc* 2004;54(6):711–26.
- McCormick RL, Lawrence R. Preliminary assessment of quality and stability of neat biodiesel in the USA. Renewable Energy Congress VII (WREC); 2004.
- McCormick RL, Graboski MS, Alleman TL, Herring AM, Tyson KS. Impact of biodiesel source material and chemical structure on emissions of criteria pollutants from a heavy-duty engine. *Environ Sci Technol* 2001;35(9):1742–7.
- Moosmüller H, Keislar RE. Vehicle Particulate Sensor System. United States Patent No. 6,542,831 2003.
- Moosmüller H, Mazzoleni C, Barber PW, Kuhns HD, Keislar RE, Watson JG. On road measurement of automotive particle emissions by ultraviolet lidar and transmissometer: instrument. *Environ Sci Technol* 2003;37(21):4971–8.
- National Research Council (U.S.A.). Committee on Vehicle Emission Inspection and Maintenance Programs. Modeling mobile-source emissions. Washington, D.C.: National Academy Press; 2000.
- National Research Council (U.S.A.). Committee on Vehicle Emission Inspection and Maintenance Programs. Evaluating vehicle emissions inspection and maintenance programs. Washington, D.C.: National Academy Press; 2001.
- NREL. Biodiesel handling and use guidelines; 2006. document available on-line at <http://www.nrel.gov/vehiclesandfuels/nrbf/pdfs/40555.pdf>.2006.
- Peterson C, Reece D. Emissions characteristics of ethyl and methyl ester of rapeseed oil compared with low sulfur diesel control fuel in a chassis dynamometer test of a pickup truck. *Trans ASAE* 1996;39(3): 805–16.
- Peterson CL, Hustrulid T. Carbon cycle for rapeseed oil biodiesel fuels. *Biomass Bioenergy* 1998;14(2):91–101.
- Peterson CL, Thompson JC, Taberski JS, Reece DL, Fleischman G. Long-range on road test with twenty-percent rapeseed biodiesel. *Appl Eng Agric* 1999;15(2):91–101.
- Pierson WR, Brachazek WW. Particulate matter associated with vehicles on the road. II. *Aerosol Sci Technol* 1983;2:1–40.
- Pope CA, Burnett RT, Thun MJ, Calle EE, Krewski D, Ito K, et al. Lung cancer, cardiopulmonary mortality, and long-term exposure to fine particulate air pollution. *JAMA-J Am Med Assoc* 2002;287(9):1132–41.
- Sagebiel JC, Zielinska B, Walsh PA, Chow JC, Cadle SH, Mulawa PA, et al. PM-10 exhaust samples collected during IM-240 dynamometer tests of in-service vehicles in Nevada. *Environ Sci Technol* 1997;31(1):75–83.
- Sharp AC, Howell S, Joe J. The effect of biodiesel fuels on transient emissions from modern diesel engines—part i: regulated emissions and performance. *SAE Tech Ser* 2000;2000-01-1967.
- Stedman DH. Automobile carbon monoxide emission. *Environ Sci Technol* 1989;23(2):147–9.
- Walsh PA, Sagebiel JC, Lawson DR, Knapp KT, Bishop GA. Comparison of auto emission measurement techniques. *Sci Total Environ* 1996;189/190:175–80.
- Zervas E, Dorlhene P, Forti L, Perrin C, Momique JC, Monier R, et al. Interlaboratory test of exhaust PM using ELPI. *Aerosol Sci Technol* 2005;39(4):333–46.